

## Developmental Localization of Nephrin in Zebrafish and Medaka Pronephric Glomerulus

**Koichiro Ichimura, Yayoi Fukuyo, Tomomi Nakamura, Rebecca Powell, Tatsuo Sakai, Ralf Janknecht, and Tomoko Obara**

Department of Cell Biology, University of Oklahoma Health Sciences Center, Oklahoma City, Oklahoma (KI, YF, TN, RPR, TO); Department of Anatomy and Life Structure, Juntendo University School of Medicine, Tokyo, Japan (KI, TS); and Department of Biological Science and Technology, Graduate School of Industrial Science and Technology, Tokyo University of Science, Noda, Chiba, Japan (TN)

### Summary

Slit diaphragm (SD) is a highly specialized intercellular junction between podocyte foot processes and plays a crucial role in the formation of the filtration barrier. In this study, we examined the developmental localization of Nephrin, an essential component of SD, in the pronephric glomerulus of zebrafish and medaka. In the mature glomerulus of both fish, Nephrin is localized along the glomerular basement membrane as seen in mammals, indicating that Nephrin is localized at the SD. Interestingly, Nephrin was detected already in immature podocytes before the SD and foot processes started to form in both fish. Nephrin was localized along the cell surface of immature podocytes but as different localization patterns. In zebrafish, Nephrin signal bordered the lateral membrane of podocytes, which were columnar in shape, as in rat immature podocytes. However, in medaka immature podocytes, Nephrin was localized in a punctate pattern among podocyte cell bodies. These findings suggest that Nephrin needs to be integrated to the membrane before the formation of the SD and then moves to the proper site to form the SD. Furthermore, a podocyte-specific marker, such as Nephrin, should be a useful tool for the future analysis of pronephric glomerular development in fish mutants and morphants. (*J Histochem Cytochem* 61:313–324, 2013)

### Keywords

pronephros, podocytes, slit diaphragm, nephrin, glomerulogenesis, zebrafish, medaka

The pronephros functions as a primary osmoregulatory organ in the larvae of teleost fish and amphibians (Howland 1916; Tytler et al. 1996). Teleost fish generally possess a pair of functional pronephroi consisting of three anatomical subunits (the glomerulus, pronephric tubule, and pronephric duct) (Drummond et al. 1998). The pronephros of small aquatic animals has been widely used to study embryonic kidney development (Drummond 2005; Wessely and Obara 2008). Among those, zebrafish and medaka are widely used because of their transparency, which is ideal for observing and manipulating organ development, in addition to the high fecundity and rapid development of internal organs.

The glomerulus exhibits a common structural organization among several taxonomic groups of vertebrates and kidney types (pronephros, mesonephros, and metanephros) (Ichimura et al. 2007) but is obviously adapted to the

different developmental and homeostatic requirements (Marshall and Smith 1930; Richter and Splechtina 1996). Structurally, the glomerulus can be divided into vascular and epithelial regions. The vascular region is the core structure of the glomerulus and consists of the capillary network and mesangium. This region is surrounded by the epithelial region, a sheet-like structure, which consists of podocytes and the glomerular basement membrane (GBM).

---

Received for publication December 8, 2012; accepted December 28, 2012.

### Corresponding Author:

Dr. Tomoko Obara, Department of Cell Biology, University of Oklahoma Health Sciences Center, 975 NE 10th St, BRC 256, Oklahoma City, OK 73104.

E-mail: tomoko-obara@ouhsc.edu

The vertebrate podocyte is an epithelial cell highly specialized for glomerular filtration. It is composed of three subcellular compartments: the cell body, the primary processes, and the foot processes (Kriz and Kaissling 2007). Podocytes adhere to the GBM primarily via their numerous foot processes, and the space between adjacent podocyte foot processes is spanned by a slit diaphragm (SD). The basic cytoarchitecture of podocytes is highly conserved throughout various types of vertebrates (Takahashi-Iwanaga 2002; Ichimura et al. 2007, 2009). Furthermore, podocytes are widely distributed among the coelomic invertebrates, and their cytoarchitecture is similar to vertebrates (Ruppert et al. 2003; Schmidt-Rhaesa 2007).

The SD is an essential element in filtration barrier function. Three kinds of SD-specific proteins—Nephrin, Podocin, and Neph1—are localized at the SD together with several tight junction-related proteins in mammals (Pavenstadt et al. 2003; Fukasawa et al. 2009). These SD-specific proteins are crucial for the formation and maintenance of the SD, and mutations in nephrin and podocin genes cause congenital nephritic syndrome of the Finnish type and autosomal recessive steroid-resistant nephrotic syndrome, respectively (Kestila et al. 1998; Boute et al. 2000). Zebrafish homologues of Nephrin and Podocin also play a crucial role in SD formation and function in the zebrafish pronephric glomerulus. Splice blocking of nephrin and podocin by morpholino antisense oligonucleotides results in a failure to form normal podocyte architecture, including regular foot processes and the SD (Kramer-Zucker et al. 2005). However, the localization of Nephrin and Podocin protein has not been investigated on a subcellular basis in pronephric glomerular development of teleost fish so far.

In the present study, to explore the developmental localization of Nephrin protein in the pronephric glomerulus of zebrafish and medaka, we developed a fish-specific anti-Nephrin antibody. We also demonstrate that immunohistochemical detection of Nephrin is useful for morphological phenotype analysis of the pronephric glomerulus in a zebrafish mutant.

## Materials and Methods

### Fish Maintenance and Stocks

Medaka *Oryzias latipes* (Cab strain) and zebrafish *Danio rerio* (wild-type AB strain, heterozygous *mpp5a*<sup>m520</sup>) (Wei and Malicki 2002) were maintained and raised at 28.5°C under a 14-hr light/10-hr dark cycle. Medaka and zebrafish embryos were kept at 28.5°C in medaka embryo culture medium (17 mM NaCl, 0.4 mM KCl, 0.3 mM CaCl<sub>2</sub>, 0.65 mM MgSO<sub>4</sub>, 0.01% methylene blue) and 0.5× E2 egg medium (7.5 mM NaCl, 0.25 mM KCl, 0.5 mM CaCl<sub>2</sub>, 0.5 mM MgSO<sub>4</sub>, 0.075 mM KH<sub>2</sub>PO<sub>4</sub>, 0.025 mM Na<sub>2</sub>HPO<sub>4</sub>, 0.35 mM NaHCO<sub>3</sub>, 0.01% methylene blue), respectively.

Embryos and larvae were staged according to hours post-fertilization (hpf) or days postfertilization (dpf). All animal experiments were performed in strict accordance with the recommendation in the Guide for the Care and Use of Laboratory Animals of the National Institutes of Health and were covered by protocols approved by the Institutional Animal Care and Use Committee of the University of Oklahoma Health Sciences Center (IACUC protocol #12-033 to TO).

### In Situ Hybridization

Zebrafish nephrin cDNA template was obtained from pCR-BluntII-TOPO-zebrafish nephrin linearized by NotI as described in Kramer-Zucker et al. (2005). Medaka partial-length nephrin cDNA was obtained by RT-PCR from total RNA isolated from 5 to 7 dpf Cab embryos using the RNAqueous-4PCR Kit (Invitrogen; Carlsbad, CA). RT-PCR was performed using the SuperScript III One-Step RT-PCR System with Platinum Taq High Fidelity (Invitrogen) followed by a second PCR using Phusion High-Fidelity DNA Polymerase (New England BioLabs; Ipswich, MA). The primers used for RT-PCR were as follows: menephrin-677F1: 5'-TGC TCA TGC TGG AGT GTG TCT-3', menephrin-1038R1: 5'-GTT GGC TGA GCA GAG CTG AAT-3'. The primers used for the second PCR were as follows: menephrin-728F2: 5'-GCT GGA GCA AGA ATG GAG AGA-3', menephrin-1825R2T7: 5'-GGT AAT ACG ACT CAC TAT AGG AGC TGA ATT CTG GTG GGT GAA-3'. The second PCR product was used as a template for the digoxigenin-labeled antisense RNA probe. All probes were synthesized using SP6 (for zebrafish nephrin) or T7 (for medaka nephrin) RNA polymerase (New England BioLabs) and DIG-RNA labeling (Roche Diagnostics; Mannheim, Germany) according to the manufacturer's instructions. Embryos were fixed in 4% paraformaldehyde, 0.1% Tween 20 in phosphate-buffered saline (PBS) for 2 hr at room temperature; changed to 100% methanol; and stored at -20°C. Whole-mount in situ hybridization was performed as described previously (Hauptmann and Gerster 2000; Thisse and Thisse 2008). Alkaline phosphatase-conjugated anti-digoxigenin (Roche Diagnostics) was used to localize the probes. NBT/BCIP (Roche Diagnostics) was used as the chromogenic substrate to produce the blue staining. After color development, samples were dehydrated in a graded series of methanol and embedded in JB-4 resin (Polysciences; Warrington, PA). Then, 5- to 7- $\mu$ m-thick sections were cut with an RN2255 microtome (Leica Microsystems; Wetzlar, Germany) and counterstained with special eosin II (BBC Biochemical; Mount Vernon, WA). After mounting in Poly-Mount (Polysciences), the stained sections were photographed on a Provis AX-70 microscope (Olympus; Tokyo, Japan) equipped with a RETIGA EXi digital camera (QImaging; Surrey, Canada).

## Antibodies

Polyclonal anti-zebrafish Nephrin antibody was raised in rabbits using its carboxy-terminal peptide RDTDLP FELRGELV (1229–1242 amino acids) coupled to KLH, as described by Ebarasi et al. (2009). The antiserum was affinity purified against the immunizing peptide (Covance; Denver, PA). Mouse monoclonal anti-rat ZO-1 (a kind gift from Drs. S. Tsukita and S. Tsukita) was raised against the fraction rich in adherence junction obtained from rat liver (Itoh et al. 1991).

## Production of Myc-Tagged Zebrafish Nephrin Intracellular Region

cDNA encoding the intracellular region of zebrafish Nephrin (amino acids 1065–1242) was generated by PCR using total RNA from 2 dpf zebrafish larvae as a template, subcloned into the pCS3<sup>+</sup>-6Myc vector, and verified by DNA sequencing. Human embryonic kidney 293T cells were seeded in 60-mm dishes and grown to a confluency of 30%. Then, they were transiently transfected by the calcium phosphate co-precipitation method with a total of 9 µg plasmid DNA (Wu and Janknecht 2002). The precipitate was left on the cells for 12 hr, after which it was removed by washing twice with 2 ml PBS. Cells were further incubated in standard medium supplemented with 10% fetal calf serum (FCS) at 37°C for 36 hr and then lysed essentially as described before by boiling in Laemmli sample buffer (Shin and Janknecht 2007). Protein lysate was subjected to SDS-PAGE, transferred to a PVDF membrane, and processed for immunoblot analysis, as previously described (Papoutsopoulou and Janknecht 2000).

## Immunohistochemistry

Whole-mount immunohistochemistry was performed as described previously (Bubenschikova et al. 2012). In brief, embryos were fixed with Dent's fixative (20% DMSO in methanol) (Dent and Klymkowsky 1989) overnight at 4°C. Fixed samples were rehydrated with a graded series of methanol and washed with PBS containing 0.5% Triton X-100 (PBSTx). For antigen retrieval, some samples were heated in PBSTx or Antigen Retrieval Reagent Universal (ARR-U; R&D Systems, Minneapolis, MN) for 15 min at 95°C on a heat block (Sawada et al. 2010; Sawada and Sun 2010). Subsequently, the samples were blocked with incubation solution (PBSTx containing 10% normal goat serum and 1% DMSO) for 2 hr at room temperature and incubated with the anti-Nephrin antibody (working dilution 1:100) diluted with incubation solution for 12 hr at 4°C. After washing with PBSTx, the samples were incubated with Alexa Fluor 546-conjugated goat anti-rabbit IgG (H+L) (Jackson ImmunoResearch Laboratories; West Grove, PA) diluted

with incubation solution (1:1000) for 2 hr at room temperature. Some samples were subsequently incubated with anti-ZO-1 antibody diluted with incubation buffer (1:100) for 12 hr at 4°C and then with Alexa Fluor 488-conjugated goat anti-mouse IgG (H+L) (Jackson ImmunoResearch Laboratories) diluted with incubation solution (1:1000) for 2 hr at room temperature. Stained samples were dehydrated in a graded series of methanol, embedded in JB-4 resin, and cut into 10-µm-thick sections with an RN2255 microtome. After mounting in antifading mounting medium (90 ml glycerol, 10 ml PBS, 100 mg p-phenylenediamine) (Platt and Michael 1983), the sections were imaged with an FV-1000 confocal laser scanning microscope (Olympus).

## Histological Analysis

Larvae were fixed with histology fixative (1.5% glutaraldehyde, 4% paraformaldehyde, 3% sucrose in 0.1 M phosphate buffer [pH 7.3]) overnight at 4°C, dehydrated in a graded series of methanol, and embedded in JB-4 resin. Then, 4-µm-thick sections were cut and stained with Harris hematoxylin and special eosin II (BBC Biochemical). The stained sections were imaged with a Provis AX-70 microscope equipped with a RETIGA EXi digital camera.

## Transmission Electron Microscopy

Embryos and larvae were immersed in histology fixative overnight at 4°C. The fixed samples were processed by a modified cold dehydration method. This method enabled detailed morphological observation of the extracellular matrices and cytoskeletons, as previously reported (Dong et al. 2010; Ichimura et al. 2010). In brief, the samples were successively immersed in 0.4% OsO<sub>4</sub> in 0.1 M phosphate buffer (pH 7.3) for 1 hr, 2% low molecular weight tannic acid (Electron Microscopy Sciences; Hatfield, PA) in 0.05 M maleate buffer for 4 hr, and 1% uranyl acetate in 0.05 M maleate buffer for 3 hr. The samples were then dehydrated in a graded series of ethanol and embedded in epoxy resin. Ultrathin silver-gold sections were produced with an ultra 45-degree diamond knife (Diatome; Biel, Switzerland) and transferred to copper grids (50 mesh; Nisshin EM, Tokyo, Japan), which had been coated with a Formvar membrane. The sections were then stained with uranyl acetate and lead citrate and observed with a JEM1230 transmission electron microscope (JEOL; Tokyo, Japan).

## Results

### Nephrin mRNA Expression in Developing Pronephric Glomerulus

Throughout pronephric development in both zebrafish and medaka, the expression pattern of nephrin strongly resembles that of Wilms tumor 1a (wt1a), which is predominantly

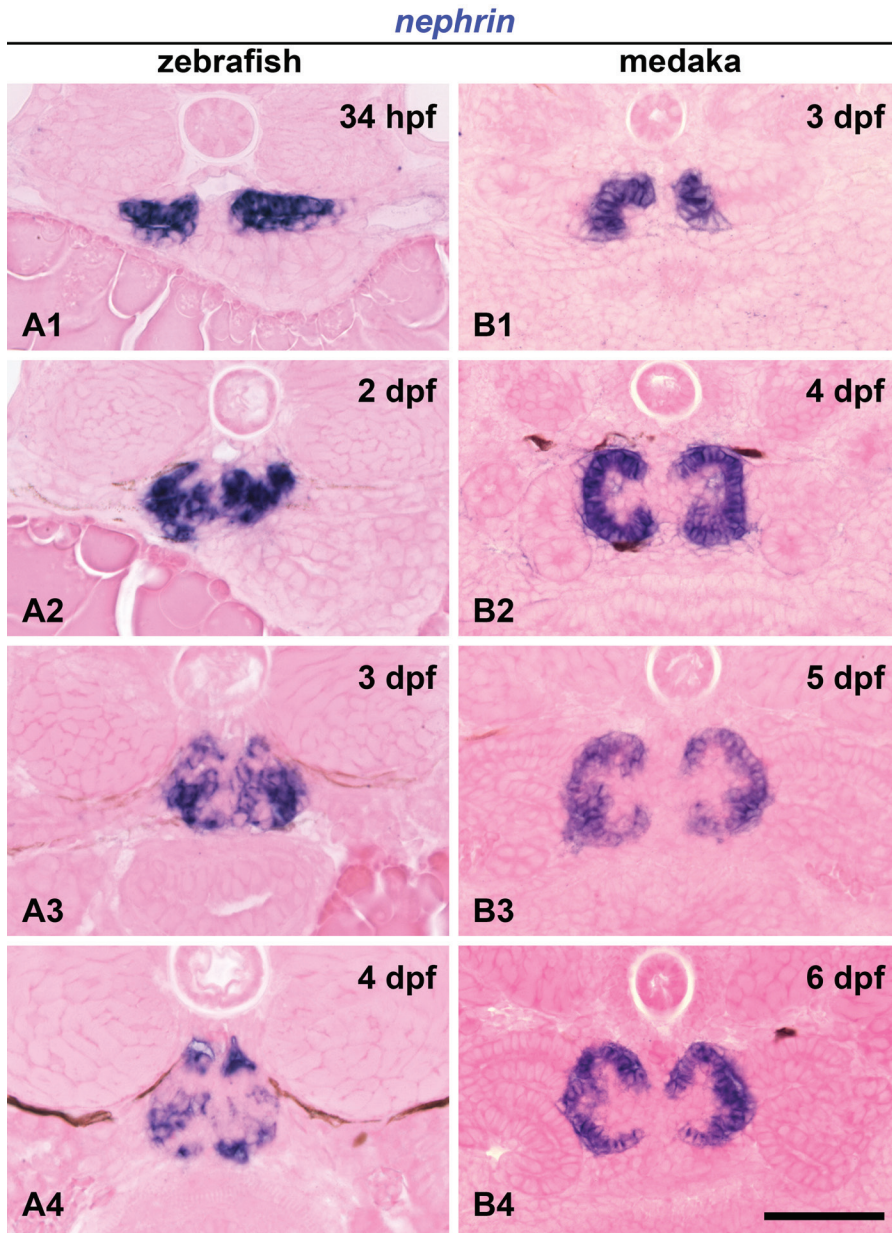


**Figure 1.** mRNA expression of nephrin in developing pronephric glomerulus. (A1–4) Zebrafish. Nephrin is expressed in the medial half of the vesicular nephron primordia as early as 34 hours postfertilization (hpf) (A1). A pair of nephrin-expressing regions is fused at the midline to form a single glomerulus by 2 days postfertilization (dpf) (A2), and its expression is preserved within the glomerulus in 3 dpf (A3) and 4 dpf (A4) embryos. (B1–4) Medaka. Nephrin-expressing regions remain separated throughout their development. Nephrin is already expressed at the most medial portion of the vesicular nephron primordia at 3 dpf (B1). Nephrin expression is found as a C-shaped epithelium at 4 dpf (B2) but has a concave and convex appearance at 5 dpf (B3) and 6 dpf (B4). Bar scale, 50  $\mu$ m.

expressed in the podocytes within the pronephric glomerulus (Drummond et al. 1998; Ichimura et al. 2012).

Expression of nephrin mRNA was detected already within the pronephric nephron primordium in 34 hpf zebrafish and 3 dpf medaka (Fig. 1A1, B1). The nephron primordia of both fish exhibited a pair of epithelial vesicles (Ichimura et al. 2012). In zebrafish, nephrin was expressed at the medial half of the pancake-shaped nephron primordia (Fig. 1A1). In medaka, nephrin expression was restricted to the most medial portion of the tube-shaped nephron primordia, which invaginates facing the lumen (Fig. 1B1).

In zebrafish, a pair of nephrin-expressing regions (the glomerular primordia) had fused at the midline to form a single glomerulus by 2 dpf (Fig. 1A2), and nephrin

expression was preserved within the glomerulus in 3 and 4 dpf embryos (Fig. 1A3, A4). On the other hand, in medaka, the nephrin-expressing regions remained separated throughout their development (Fig. 1B1–4). They exhibited a regular C-shaped epithelium at 4 dpf (Fig. 1B2) but developed additional concave and convex folds as the glomerulus matured (Fig. 1B3, B4).

#### *Specificity of Anti-Zebrafish Nephrin Antibody*

To examine the localization of Nephrin in zebrafish pronephric glomerulus, we developed an anti-zebrafish Nephrin polyclonal antibody in rabbits using the carboxy-terminal 15 amino acids, based on the previous report (Ebarasi et al.

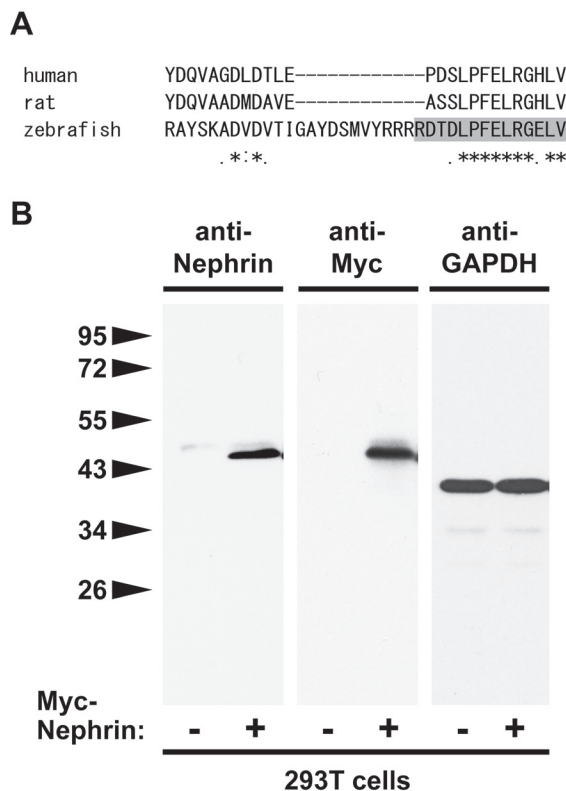


**Figure 2.** Specificity of anti-Nephrin antibody. (A) ClustalW alignment of the carboxy-terminal amino acid sequence of human, rat, and zebrafish Nephrin. Ten amino acids of its carboxy-terminus are highly conserved among these species. Polyclonal anti-zebrafish Nephrin antibody was raised using its carboxy-terminal peptide RDTDLPEFELRGELV (1228–1242 amino acids). (B) Immunoblot analysis shows that the anti-zebrafish Nephrin antibody detects a ~45-kDa band protein that corresponds with a Myc-tagged intercellular region of zebrafish Nephrin, both expressed in 293T cells. Immunoblot for GAPDH shows an equivalent amount of protein was loaded from transfected and untransfected samples.

2009). This peptide includes a 10–amino acid sequence highly conserved among human, rat, and zebrafish (Fig. 2A). To examine the specificity of the new antibody, we tested whether it was capable of reacting with a Myc-tagged intracellular region of zebrafish Nephrin expressed in 293T cells. Immunoblot analysis showed that the anti-Nephrin antibody could detect a ~45-kDa protein, corresponding to the Myc-tagged Nephrin intracellular region (Fig. 2B).

#### Efficacy of Heat-Induced Antigen Retrieval for Immunohistochemical Detection of Nephrin

To test whether the anti-Nephrin antibody was able to detect podocytes in the pronephric glomerulus, we performed whole-mount immunohistochemistry on 4 dpf zebrafish and 7 dpf medaka larvae fixed in Dent's fixative using three different protocols, as summarized in Fig. 3.

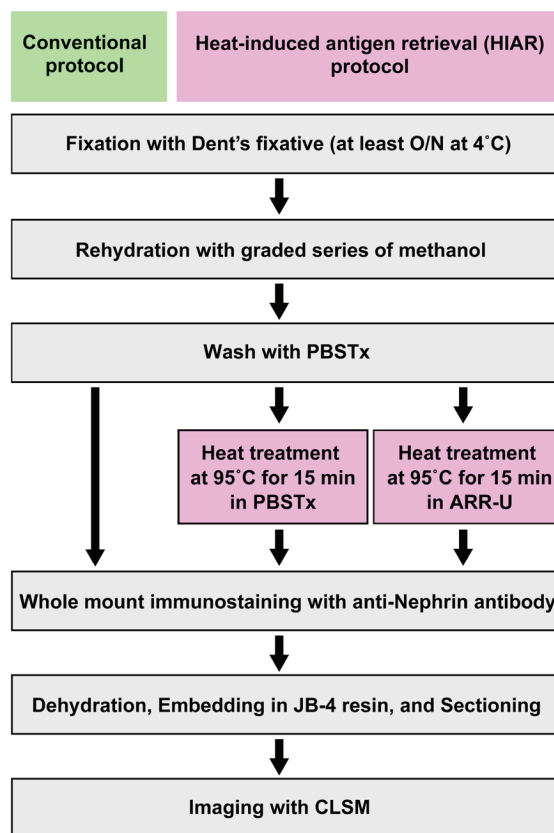


**Figure 3.** Antigen retrieval protocol for Dent's fixative-fixed samples. Heat treatment was adopted as antigen retrieval and performed at 95°C for 15 min on a heat block after washing following rehydration. We tested two types of buffer for heat treatment: phosphate-buffered saline containing Triton X-100 (PBSTx) and Antigen Retrieval Reagent Universal (ARR-U). CLSM, confocal laser scanning microscope; O/N, overnight.

Faint immunoreactivity could be detected at the glomerular region in both zebrafish and medaka processed with our conventional protocol without antigen retrieval (Fig. 4A1, B1); however, heat-induced antigen retrieval (HIAR) greatly improved the antigenicity for Nephrin, and strong immunoreactivity in the glomerulus along the GBM was recognized in both fish (Fig. 4A2, A3, B2, B3). We tested two types of buffer, PBSTx and ARR-U, in the HIAR process. In zebrafish, the recovery of Nephrin antigenicity was enhanced by the use of ARR-U compared with PBSTx (Fig. 4A2, A3). But in medaka, the efficacy was similar for both buffers (Fig. 4B2, B3). In the following immunostaining, we thus used ARR-U buffer in the HIAR process.

#### Nephrin Localization in Developing Pronephric Glomerulus

We examined the localization of Nephrin protein during the pronephric glomerular development in 34 hpf to 4 dpf zebrafish (Fig. 5) and 3 to 7 dpf medaka (Fig. 6).

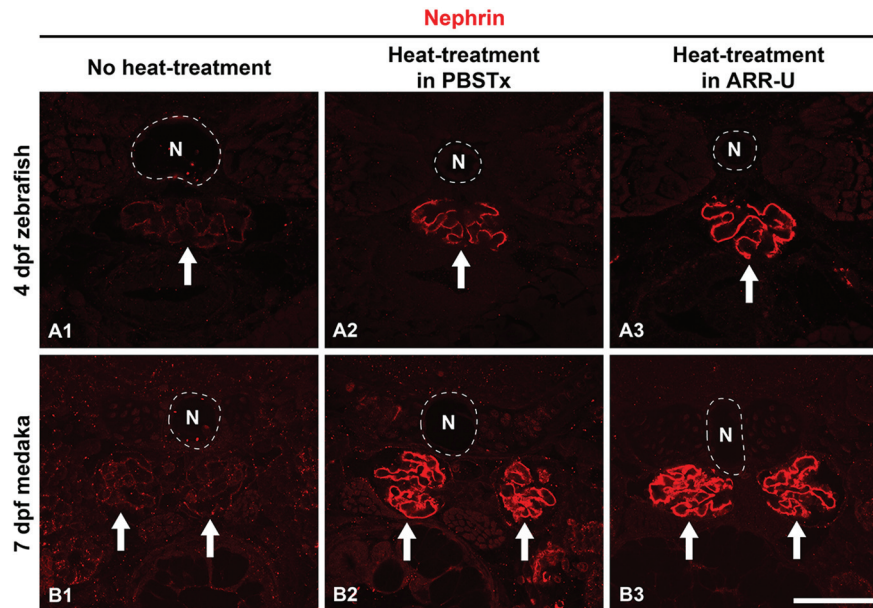


**Figure 4.** Efficacy of antigen retrieval in whole-mount immunostaining. We checked whether the anti-Nephrin antibody could detect the pronephric podocytes in 4 days postfertilization (dpf) zebrafish (A1–3) and 7 dpf medaka (B1–3) under three different conditions, which are summarized in Fig. 3. Faint immunoreactivity is found at the glomerular region both in the zebrafish and medaka processed with our conventional protocol (A1, B1). Heat-induced antigen retrieval greatly improved the antigenicity for Nephrin, and strong immunoreactivity along the glomerular basement membrane was recognized in both fish. In zebrafish, recovery of antigenicity for Nephrin was improved by the use of Antigen Retrieval Reagent Universal (ARR-U) rather than phosphate-buffered saline containing 0.5% Triton X-100 (PBSTx) (A2, A3). In medaka, both buffers had similar efficacy (B2, B3). Arrows, pronephric glomerulus. N, notochord. Bar scale, 50  $\mu$ m.

In the zebrafish, we performed double immunofluorescence labeling to assay for localization of Nephrin and ZO-1, a tight junction protein that is localized at the foot processes of zebrafish pronephric podocytes (Ichimura et al. 2012). In 34 hpf zebrafish, expression of Nephrin was not recognized at the pronephric glomerular primordia, whereas the anti-ZO-1 antibody labeled the apical tight junctions in these cells (Fig. 5A1–A3). The amorphous appearance of Nephrin immunoreactivity was found within the glomerular primordia at 40 hpf (Fig. 5B1–B3). At 2 dpf (48 hpf), immunoreactivity for Nephrin was stronger and was recognized as discontinuous tortuous lines within the glomerular region (Fig. 5C1–C3). In addition to the linear signals, Nephrin was often found along the cell membrane of the podocyte cell body (Fig. 5C1'). By 3 dpf, immunoreactivity for Nephrin was clearly recognized as two continuous tortuous lines, which were likely along the GBM (Fig. 5D1–D3). This pattern was preserved at 4 dpf (Fig. 5E1–E3). A similar tortuous linear pattern for Nephrin localization was also reported for the rodent metanephric glomerulus (Ruotsalainen et al. 1999; Kawachi et al. 2000). Nephrin immunoreactivity was not found along the apical surface membrane of the podocyte cell body after 3 dpf (Fig. 5D1').

In the medaka, the anti-ZO-1 antibody used above did not provide a sufficient immunohistochemical signal in embryos; we thus performed immunofluorescence labeling with Nephrin alone. Protein expression of Nephrin was

already present at the invaginated portion of nephron primordia in 3 dpf medaka (Fig. 6A). At 4 dpf, conspicuous immunoreactivity for Nephrin was found as a speckled pattern along the lateral membranes of the podocyte cell body, which was columnar in shape (Fig. 6B, B'). At 5 to 6 dpf, in addition to the speckled signals, Nephrin immunoreactivity was also found as discontinuous tortuous lines along the GBM (Fig. 6C, C', D, D'). At 7 dpf, by which time the foot processes are fully formed (Ichimura et al. 2012), the immunoreactivity for Nephrin was clearly recognized as two continuous tortuous lines that were likely running along the GBM but was not found at the podocyte cell body (Fig. 6E, E').

A difference in the immunoreactivity pattern for Nephrin was found in the columnar-shaped immature podocytes between zebrafish and medaka: a linear pattern in zebrafish (Fig. 5C1') and a speckled pattern in medaka (Fig. 6B', C', D', E'), as above described. To explain the discrepancy, we examined the surface ultrastructure of the podocyte cell body. In immature podocytes of medaka, a variety of microvillus-like processes were protruded from the apical membrane of the podocyte cell body, and the tips of these processes were occasionally connected via an SD-like structure (Fig. 7B, C). Such microvillus-like processes connected with the SD-like structure were not found in zebrafish (Fig. 7A). It is therefore likely that Nephrin was localized at the SD-like structure in immature podocytes of medaka.

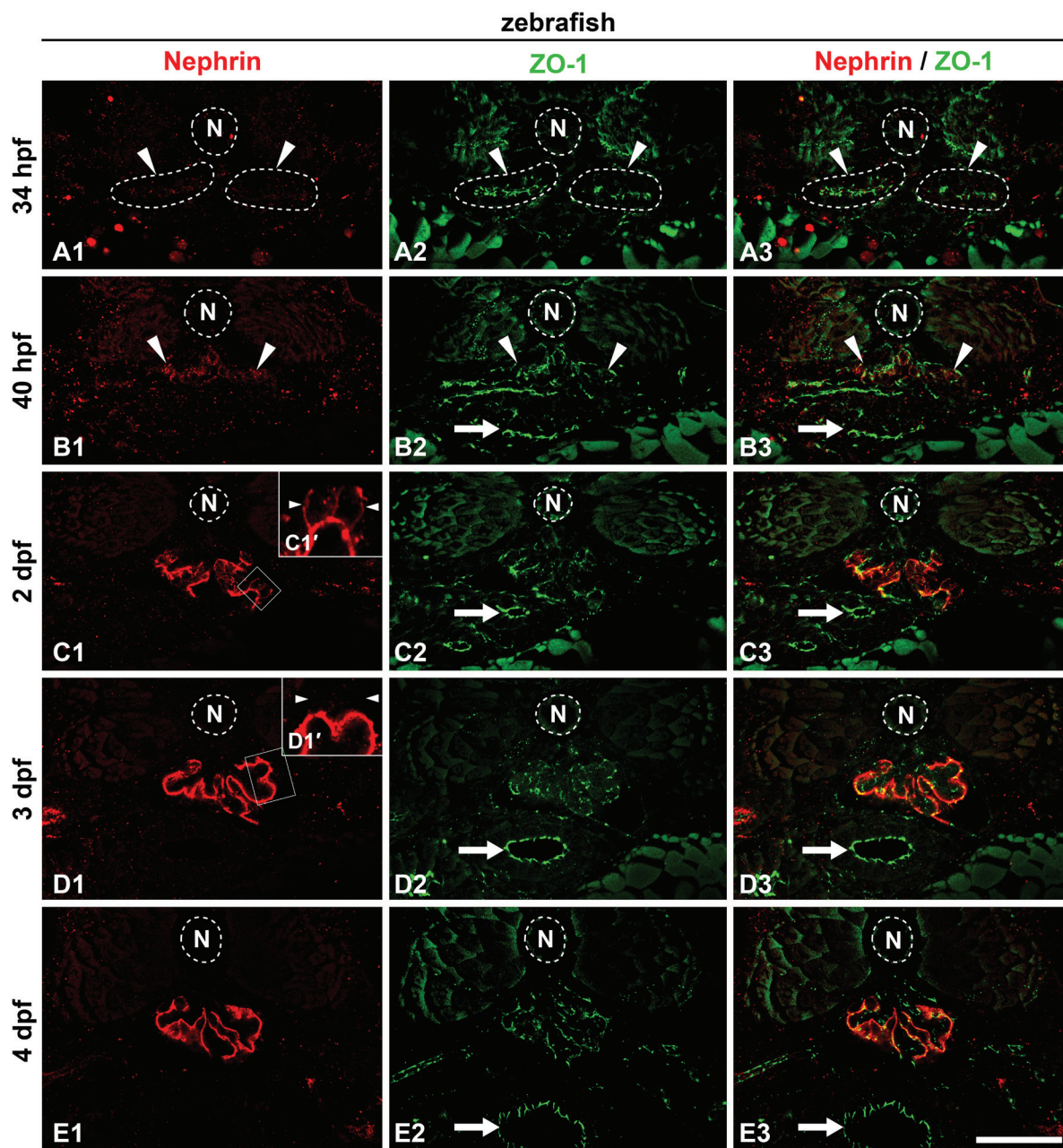
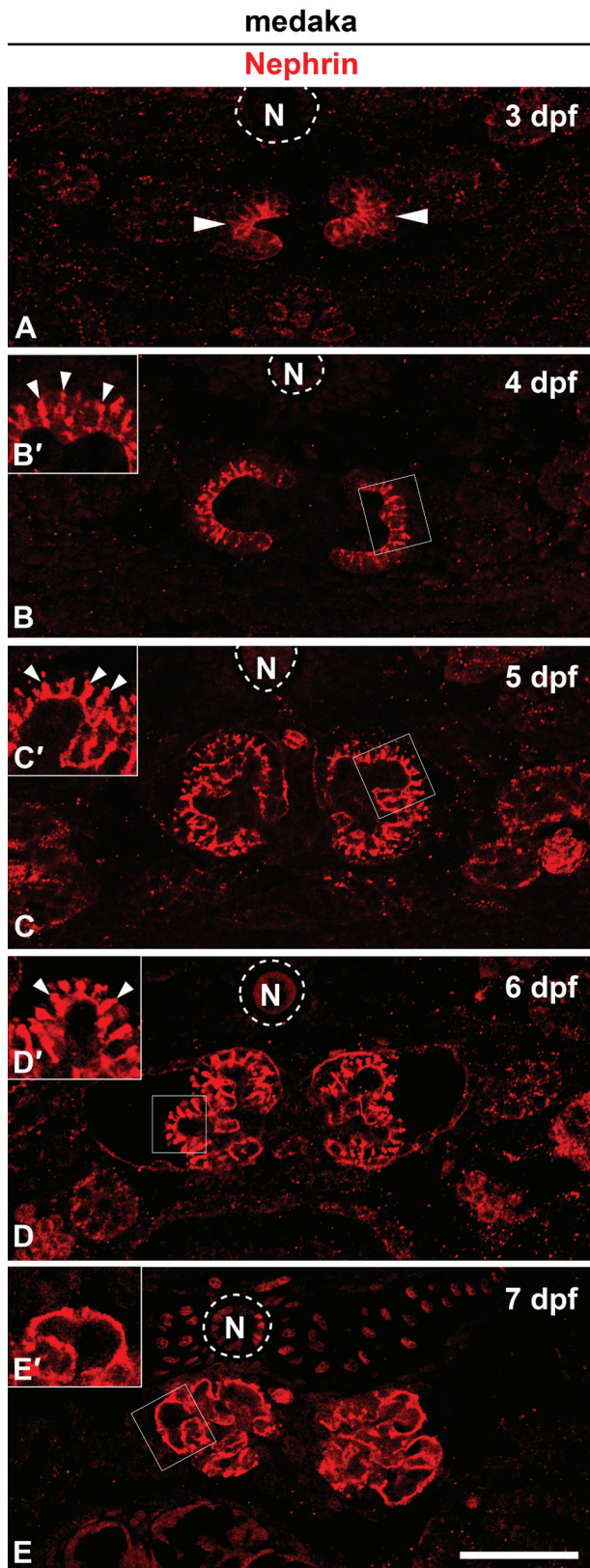


**Figure 5.** Localization of Nephrin protein in zebrafish pronephric glomerulus. Double immunofluorescence staining for Nephrin (A1, B1, C1, D1, E1; red) and the tight junction protein ZO-1 (A2, B2, C3, C4, C5; green). (A1–3) At 34 hours postfertilization (hpf), Nephrin is not detected at the pronephric glomerular primordia (arrowheads). (B1–3) At 40 hpf, weak immunoreactivity for Nephrin is initially detected with an amorphous appearance within the glomerular primordia at 40 hpf (arrowheads). (C1–3) At 2 days postfertilization (dpf), immunoreactivity for Nephrin appears in discontinuous tortuous lines at the glomerular region. In addition to the linear signals, it is often found along the cell membrane of podocyte cell body (arrowheads in C1'). (D1–3) At 3 dpf, Nephrin is clearly recognized as two continuous tortuous lines along the glomerular basement membrane. No signal is found at the podocyte cell body (arrowheads in D1'). (E1–3) At 4 dpf, Nephrin localization is identical to that at 3 dpf. Insets (C1', D1') are magnification of the field indicated by the rectangles. Arrows, tight junctions in gastrointestinal tract. N, notochord. Bar scale, 50  $\mu$ m.

#### Immunohistochemical Identification of Podocytes Using Anti-Nephrin Antibody in Zebrafish Mutant

Recently, we reported the morphological analysis of the pronephric glomerular disorganization in the zebrafish

*mpp5a/nagie oko<sup>m520</sup>* mutant (Ichimura, Fukuyo, et al. 2012). In this mutant, normal glomerular architecture is seriously disrupted. In particular, a pair of glomerular primordia failed to merge at the midline, and glomerular capillary and mesangium were not formed at all (Fig. 8A1,B1).



Consequently, it is difficult to identify the podocytes in this mutant by means of conventional histological staining. In the *mpp5a<sup>m520</sup>* mutant, the epithelioid cell masses, which were in direct contact with the extremely dilated aorta beneath the notochord, were constantly found at the level of the pectoral fin buds (Fig. 8B1). We could not determine whether these cell masses were made by podocytes on the basis of conventional light-microscopic observation. However, the anti-Nephrin antibody specifically labeled them, and thus these cell masses were identified as podocytes (Fig. 8B2).

Interestingly, localization of Nephrin within the podocytes was quite different between wild type and the *mpp5a<sup>m520</sup>* mutant. As described above, in wild type zebrafish, the immunoreactivity for Nephrin was recognized as two tortuous line segments along the GBM (Fig. 8A2, A2'), which suggested that Nephrin was localized at the foot processes of podocytes. However, Nephrin immunoreactivity was broadly distributed along the entire surface of the podocyte cell body in the mutant (Fig. 8B2, B2').

## Discussion

### Antigen Retrieval for Fish Immunohistochemistry

A variety of antigen retrieval techniques have been widely applied as a pretreatment for immunohistochemical staining on formalin-fixed, paraffin-embedded tissue sections in diagnostic pathology and analytical morphology (Shi et al. 1997; Shi and Taylor 2010). Inoue and Wittbrodt (2011) recently reported the efficacy of HIAR on formaldehyde-fixed larvae of zebrafish and medaka. The HIAR protocol has appreciably improved the immunostaining of important markers of neuronal and progenitor/stem cells, in both zebrafish and medaka, including proliferation cell nuclear



**Figure 6.** Localization of Nephrin protein in medaka pronephric glomerulus. (A) At 3 days postfertilization (dpf). Protein expression of Nephrin is already apparent at the invaginated portion of nephron primordia (arrowheads). (B, B') At 4 dpf, conspicuous immunoreactivity for Nephrin is found as a speckled pattern between the cell bodies of immature podocytes (arrowheads in B'). (C, C', D, D') At 5 to 6 dpf, in addition to the speckled signals (arrowheads in C' D'), Nephrin also occurs as discontinuous tortuous lines along the glomerular basement membrane. (E, E') By 7 dpf, immunoreactivity for Nephrin is clearly recognized as two continuous tortuous lines and is not found along the surface of podocyte cell bodies (arrowheads in E'). Insets (B', C', D', E') are magnification of the field indicated by the rectangles. N, notochord. Bar scale, 50  $\mu$ m.



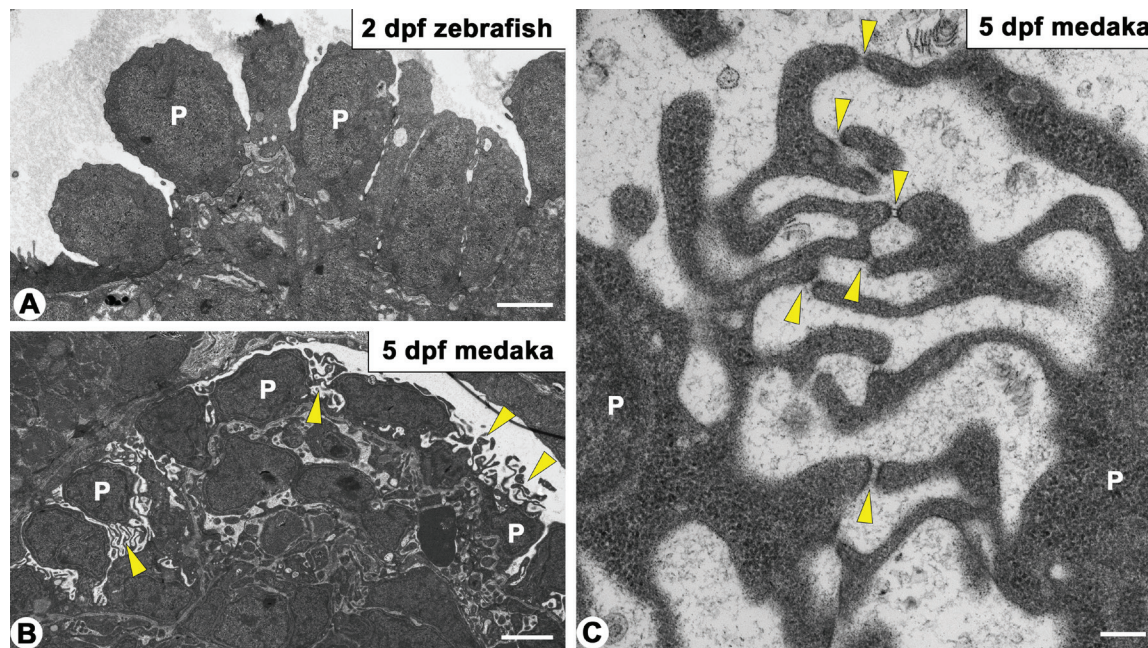


**Figure 7.** Transmission electron micrographs showing immature podocytes in zebrafish and medaka pronephric glomerulus. (A) In 2 days postfertilization (dpf) zebrafish, immature podocytes are columnar in shape. (B, C) In 5 dpf medaka, microvillus-like processes are found between the cuboidal podocytes (arrowheads in B). Slit diaphragm-like structures span the tips between these processes (arrowheads in C). P, cell body of immature podocyte. Bar scale, 2  $\mu$ m in A, B; 200 nm in C.

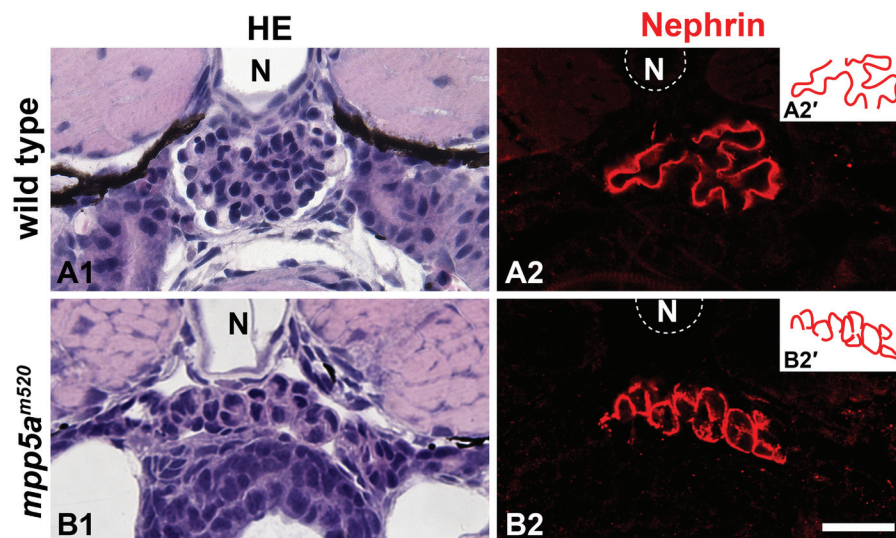


**Figure 8.** Nephrin localization in zebrafish *mpp5a<sup>m520</sup>* mutant. (A1, B1) Hematoxylin and eosin staining. In the 4 days postfertilization (dpf) zebrafish *mpp5a<sup>m520</sup>* mutant, pronephric glomerular architecture is disrupted (B1), in comparison with the 4 dpf wild type (A1). The epithelioid cell mass is constantly found beneath the notochord. (A2, B2) Nephrin immunostaining. In wild type (A2), Nephrin is clearly recognized as two tortuous line segments, but no signal is found along the entire surface of the podocyte cell body. On the other hand, in the *mpp5a<sup>m520</sup>* mutant, Nephrin is specifically found along the cell mass as a botryoidally aggregated pattern (B2). Insets (A2', B2') schematically show the topological pattern of Nephrin immunoreactivity. N, notochord. Bar scale, 50  $\mu$ m.

antigen, phosphohistone H3, glutamine synthetase, HuC/D, and PKC $\alpha$ .

In the field of developmental biology, investigators researching non-mammalian vertebrates, including zebrafish, frequently select methanol-based Dent's fixative (Dent and

Klymkowsky 1989) for whole-mount immunohistochemistry of embryos, larvae, and isolated organs (Sedmera et al. 2003; Zhou et al. 2010; Sullivan-Brown et al. 2011). However, little has been reported concerning the application of the antigen retrieval protocol for Dent's fixative-fixed samples except for

several studies by Sawada and colleagues (Sawada et al. 2010; Sawada and Sun 2010). They applied a simple HIAR protocol with ARR-U to whole-mount immunostaining of the cerebellar cortex in rodents. By the using HIAR, we also could drastically improve the immunoreactivity for the anti-Nephrin antibody and were successful in determining the localization of Nephrin in both zebrafish and medaka pronephroi. Thus, the HIAR protocol is also a valuable method for immunostaining of Dent's fixative-fixed fish samples and will be used alongside other antibodies in future research.

### *Developmental Localization of Nephrin in Pronephric Glomerulus*

To date, the localization of Nephrin protein in the developing glomerulus has been reported in the metanephros of mouse (Holzman et al. 1999), rat (Kawachi et al. 1995), and human (Ruotsalainen et al. 2000). Intriguingly, protein expression of Nephrin is already recognizable in the immature podocytes of these mammals before the stage when the foot processes and SD form. In the immature columnar podocytes at the rat S-shaped body stage, the immunoreactivity for Nephrin was found along the basolateral membrane below the apical junctional complex (Kawachi et al. 1995). In zebrafish pronephros, Nephrin was also found as a linear pattern along the surface membrane of the cell body in immature podocytes before the stage when the foot processes and SD appear (3–4 dpf in zebrafish) (Drummond et al. 1998; Ferrante et al. 2009). These findings indicate that Nephrin needs to be integrated to the membrane before the formation of the SD and then gathers at the proper site to form the SD.

The junctional complex of immature podocytes migrates along the lateral cell surface toward the basal side of the cell, after which the apical membrane domain of podocytes becomes considerably expanded. During this process, some patches of intercellular junctions, which sometimes have a ladder-like appearance, temporarily remain in the apical membrane region of the cell body (Reeves et al. 1978), and Nephrin is also recognized at these junctions in human (Ruotsalainen et al. 2000). In pronephric podocytes of zebrafish and medaka, such ladder-like junctions were not found; however, in medaka, SD-like structures were found between the tips of microvillus-like processes protruding from the apical surface of the podocyte cell body. In medaka, the immunoreactivity for Nephrin was recognized as speckled signals along the side membrane of the podocyte cell body. These speckled signals likely corresponded to the SD-like structure, but the functional significance of the structure is not clearly understood.

The SD-like structures were not found in the normal zebrafish podocytes that we observed, although we cannot completely eliminate the possibility that SD-like structures may be briefly present during normal glomerulogenesis in zebrafish

pronephros because podocyte differentiation occurs over a much shorter period of time in zebrafish than in medaka.

Finally, the immunoreactivity for Nephrin was only present as tortuous lines along the GBM both in zebrafish and medaka pronephric glomerulus, as seen in rodent and human metanephros (Holzman et al. 1999; Ruotsalainen et al. 1999, 2000). This fact indicated that Nephrin protein is also exclusively localized at the foot processes in zebrafish and medaka mature podocytes.

### *Usefulness of Immunohistochemical Detection of Nephrin in Morphological Analysis of Pronephric Glomerulogenesis*

In zebrafish, several forms of pronephric glomerular disorganization have been reported previously and can be topologically classified into three types:

1. Septal type, which is often associated with cystic dilatation of the Bowman's capsule or pronephric tubule. In this type, the pronephric glomerulus is recognized as a septum between the cysts, as found in a variety of cystic mutants (Drummond et al. 1998; Zhao and Malicki 2007; Sullivan-Brown et al. 2008).
2. Flattened type, which is interpreted as a hypoplastic glomerulus consisting of a glomerular capillary and mesangium, as found in some nephrin knockdown models and in the zebrafish mosaic eye (moe) mutant (Kramer-Zucker et al. 2005)
3. Vesicular type, in which the glomerulus has retained a primitive vesicular structure, coupled with agenesis of the glomerular capillary and mesangium, and is recognized as paired vesicles (Serluca et al. 2002; Müller et al. 2011; Ichimura et al. 2012)

The normal glomerular architecture is remarkably perturbed, particularly in the septal and vesicular types and, in such a disorganized glomerulus, it is difficult to identify the podocytes by conventional light microscopy. Fortunately, the anti-Nephrin antibody developed in this study was able to clearly visualize the podocytes and readily determine their position in the *mpp5a<sup>m520</sup>* mutant, in which the pronephric glomerular architecture is disrupted and exhibits vesicular-type disorganization (Ichimura et al. 2012).

In the 4 dpf *mpp5a<sup>m520</sup>* mutant, a unique pattern of Nephrin immunoreactivity was found in the podocytes. As mentioned above, in the 4 dpf normal larvae, the immunoreactivity for Nephrin was recognized as a pair of tortuous line segments along the GBM, but no signal was found in the cell body. Unlike in the wild type, the *mpp5a<sup>m520</sup>* mutants exhibited the Nephrin immunoreactivity along the entire

margin of the cell body. Thus, the glomerulus stained with this antibody appeared as botryoidal aggregation. Previous electron microscopic studies have revealed a number of microvillus-like processes, which were connected to each other via SD-like structures and protruded from the apical surface of the podocyte cell body in the *mpp5a<sup>m520</sup>* mutants (Ichimura et al. 2012), as well as in normal medaka. Thus, the signal along the cell body margin is likely to correspond to the SD-like structures.

In conclusion, developmental expression of nephrin mRNA and localization of its protein are now clearly understood in the zebrafish and medaka pronephric glomerulus. Furthermore, the development of a podocyte-specific antibody, such as the anti-Nephrin antibody presented here, should be a useful tool for the future analysis of pronephric glomerular development in fish mutants and morphants.

### Acknowledgment

The authors thank Drs. Deborah Garrity and Hiroyuki Matsumoto for helpful criticism and comments on the manuscript. The anti-ZO-1 antibody was provided by Drs. Shoichiro Tsukita and Sachiko Tsukita. The authors also thank Drs. Daigo Inoue and Joachim Wittbrodt for giving us some useful information about antibody.

### Declaration of Conflicting Interests

The author(s) declared no potential conflicts of interest with respect to the research, authorship, and/or publication of this article.

### Funding

The author(s) disclosed receipt of the following financial support for the research, authorship, and/or publication of this article: TO acknowledges financial support from the University of Oklahoma Health Sciences Center (OUHSC). KI was supported by Grants-in-Aid for Scientific Research from the Ministry of Education, Culture, Sports, Science and Technology of Japan (No. 23590226). TO was supported by NIH grants R21-DK069604 and R01-DK078209.

### References

- Boute N, Gribouval O, Roselli S, Benessy F, Lee H, Fuchshuber A, Dahan K, Gubler MC, Niaudet P, Antignac C. 2000. NPHS2, encoding the glomerular protein podocin, is mutated in autosomal recessive steroid-resistant nephrotic syndrome. *Nat Genet.* 24:349–354.
- Bubenshchikova E, Ichimura K, Fukuyo Y, Powell R, Hsu C, Morrical SO, Sedor JR, Sakai T, Obara T. 2012. *Wtip* and *Vangl2* are required for mitotic spindle orientation and cloaca morphogenesis. *Biol Open.* 1:588–596.
- Dent JA, Klymkowsky MW. 1989. Whole-mount analyses of cytoskeletal reorganization and function during oogenesis and early embryogenesis in *Xenopus*. In: Schatten H, Schatten G, editors. *The cell biology of fertilization*. New York: Academic Press. p. 63–103.
- Dong HM, Ichimura K, Sakai T. 2010. Structural organization of hepatic portal vein in rat with special reference to musculature, intimal folds, and endothelial cell alignment. *Anat Rec (Hoboken).* 293:1887–1895.
- Drummond IA. 2005. Kidney development and disease in the zebrafish. *J Am Soc Nephrol.* 16:299–304.
- Drummond IA, Majumdar A, Hentschel H, Elger M, Solnica-Krezel L, Schier AF, Neuhauss SC, Stemple DL, Zwartkruis F, Rangini Z, et al. 1998. Early development of the zebrafish pronephros and analysis of mutations affecting pronephric function. *Development.* 125:4655–4667.
- Ebarasi L, He L, Hultenby K, Takemoto M, Betsholtz C, Trygvason K, Majumdar A. 2009. A reverse genetic screen in the zebrafish identifies *crb2b* as a regulator of the glomerular filtration barrier. *Dev Biol.* 334:1–9.
- Ferrante MI, Romio L, Castro S, Collins JE, Goulding DA, Stemple DL, Woolf AS, Wilson SW. 2009. Convergent extension movements and ciliary function are mediated by *ofd1*, a zebrafish orthologue of the human oral-facial-digital type 1 syndrome gene. *Hum Mol Genet.* 18:289–303.
- Fukasawa H, Bornheimer S, Kudlicka K, Farquhar MG. 2009. Slit diaphragms contain tight junction proteins. *J Am Soc Nephrol.* 20:1491–1503.
- Hauptmann G, Gerster T. 2000. Multicolor whole-mount in situ hybridization. *Methods Mol Biol.* 137:139–148.
- Holzman LB, St John PL, Kovari IA, Verma R, Holthofer H, Abrahamson DR. 1999. Nephrin localizes to the slit pore of the glomerular epithelial cell. *Kidney Int.* 56:1481–1491.
- Howland RB. 1916. On the effect of removal of the pronephros of the amphibian embryo. *Proc Natl Acad Sci U S A.* 2:231–234.
- Ichimura K, Bubenshchikova E, Powell R, Fukuyo Y, Nakamura T, Tran U, Oda S, Tanaka M, Wessely O, Kurihara H, et al. 2012. A comparative analysis of glomerulus development in the pronephros of medaka and zebrafish. *PLoS One.* 7:e45286.
- Ichimura K, Fukuyo Y, Nakamura T, Powell R, Sakai T, Obara T. 2012. Structural disorganization of pronephric glomerulus in zebrafish *mpp5a/nagie oko* mutant. *Dev Dyn.* 241:1922–1932.
- Ichimura K, Kurihara H, Sakai T. 2007. Actin filament organization of foot processes in vertebrate glomerular podocytes. *Cell Tissue Res.* 329:541–557.
- Ichimura K, Kurihara H, Sakai T. 2009. Beta-cytoplasmic actin localization in vertebrate glomerular podocytes. *Arch Histol Cytol.* 72:165–174.
- Ichimura K, Kurihara H, Sakai T. 2010. Primary cilia disappear in rat podocytes during glomerular development. *Cell Tissue Res.* 341:197–209.
- Inoue D, Wittbrodt J. 2011. One for all—a highly efficient and versatile method for fluorescent immunostaining in fish embryos. *PLoS One.* 6:e19713.
- Itoh M, Yonemura S, Nagafuchi A, Tsukita S, Tsukita S. 1991. A 220-kD undercoat-constitutive protein: its specific localization at cadherin-based cell-cell adhesion sites. *J Cell Biol.* 115:1449–1462.
- Kawachi H, Abrahamson DR, St John PL, Goldstein DJ, Shia MA, Matsui K, Shimizu F, Salant DJ. 1995. Developmental expression

- of the nephritogenic antigen of monoclonal antibody 5-1-6. *Am J Pathol.* 147:823–833.
- Kawachi H, Koike H, Kurihara H, Yaoita E, Orikasa M, Shia MA, Sakai T, Yamamoto T, Salant DJ, Shimizu F. 2000. Cloning of rat nephrin: expression in developing glomeruli and in proteinuric states. *Kidney Int.* 57:1949–1961.
- Kestila M, Lenkkeri U, Mannikko M, Lamerdin J, McCready P, Putaala H, Ruotsalainen V, Morita T, Nissinen M, Herva R, et al. 1998. Positionally cloned gene for a novel glomerular protein—nephrin—is mutated in congenital nephrotic syndrome. *Mol Cell.* 1:575–582.
- Kramer-Zucker AG, Wiessner S, Jensen AM, Drummond IA. 2005. Organization of the pronephric filtration apparatus in zebrafish requires Nephrin, Podocin and the FERM domain protein Mosaic eyes. *Dev Biol.* 285:316–329.
- Kriz W, Kaissling B. 2007. Structural organization of the mammalian kidney. In: Alpern RJ, Hebert SC, editors. *Seldin and Giebisch's The kidney—physiology and pathophysiology.* New York: Academic Press. p. 479–563.
- Marshall EK, Smith HW. 1930. The glomerular development of the vertebrate kidney in relation to habitus. *Biol Bull.* 59:135–153.
- Müller T, Rumpel E, Hradetzky S, Bollig F, Wegner H, Blumenthal A, Greinacher A, Endlich K, Endlich N. 2011. Non-muscle myosin IIA is required for the development of the zebrafish glomerulus. *Kidney Int.* 80:1055–1063.
- Papoutsopoulou S, Janknecht R. 2000. Phosphorylation of ETS transcription factor ER81 in a complex with its coactivators CREB-binding protein and p300. *Mol Cell Biol.* 20:7300–7310.
- Pavenstadt H, Kriz W, Kretzler M. 2003. Cell biology of the glomerular podocyte. *Physiol Rev.* 83:253–307.
- Platt JL, Michael AF. 1983. Retardation of fading and enhancement of intensity of immunofluorescence by p-phenylenediamine. *J Histochem Cytochem.* 31:840–842.
- Reeves W, Caulfield JP, Farquhar MG. 1978. Differentiation of epithelial foot processes and filtration slits: sequential appearance of occluding junctions, epithelial polyanion, and slit membranes in developing glomeruli. *Lab Invest.* 39:90–100.
- Richter S, Splechtma H. 1996. The structure of anuran podocyte—determined by ecology? *Acta Zoologica.* 77:335–348.
- Ruotsalainen V, Ljungberg P, Wartiovaara J, Lenkkeri U, Kestila M, Jalanko H, Holmberg C, Tryggvason K. 1999. Nephrin is specifically located at the slit diaphragm of glomerular podocytes. *Proc Natl Acad Sci U S A.* 96:7962–7967.
- Ruotsalainen V, Patrakka J, Tissari P, Reponen P, Hess M, Kestila M, Holmberg C, Salonen R, Heikinheimo M, Wartiovaara J, et al. 2000. Role of Nephrin in cell junction formation in human nephrogenesis. *Am J Pathol.* 157:1905–1916.
- Ruppert E, Fox R, Barnes R. 2003. *Invertebrate zoology.* Belmont, CA: Thomson Learning.
- Sawada K, Sakata-Haga H, Fukui Y. 2010. Alternating array of tyrosine hydroxylase and heat shock protein 25 immunopositive Purkinje cell stripes in zebrin II-defined transverse zone of the cerebellum of rolling mouse Nagoya. *Brain Res.* 1343:46–53.
- Sawada K, Sun XZ. 2010. Application of heat-induced antigen retrieval on whole mount immunostaining for adult mouse cerebellum. *Curr Neurobiol.* 1:21–24.
- Schmidt-Rhaesa A. 2007. Excretory system. In: *The evolution of organ systems.* New York: Oxford University Press. p. 169–190.
- Sedmera D, Reckova M, deAlmeida A, Sedmerova M, Biermann M, Volejnik J, Sarre A, Raddatz E, McCarthy RA, Gourdie RG, et al. 2003. Functional and morphological evidence for a ventricular conduction system in zebrafish and *Xenopus* hearts. *Am J Physiol Heart Circ Physiol.* 284:H1152–H1160.
- Serluca FC, Drummond IA, Fishman MC. 2002. Endothelial signaling in kidney morphogenesis: a role for hemodynamic forces. *Curr Biol.* 12:492–497.
- Shi SR, Cote RJ, Taylor CR. 1997. Antigen retrieval immunohistochemistry: past, present, and future. *J Histochem Cytochem.* 45:327–343.
- Shi SR, Taylor CR. 2010. Antigen retrieval immunohistochemistry based research and diagnostics. Hoboken, NJ: John Wiley.
- Shin S, Janknecht R. 2007. Diversity within the JMJD2 histone demethylase family. *Biochem Biophys Res Commun.* 353:973–977.
- Sullivan-Brown J, Bisher ME, Burdine RD. 2011. Embedding, serial sectioning and staining of zebrafish embryos using JB-4 resin. *Nat Protoc.* 6:46–55.
- Sullivan-Brown J, Schottenfeld J, Okabe N, Hostetter CL, Serluca FC, Thiberge SY, Burdine RD. 2008. Zebrafish mutations affecting cilia motility share similar cystic phenotypes and suggest a mechanism of cyst formation that differs from *pkd2* morphants. *Dev Biol.* 314:261–275.
- Takahashi-Iwanaga H. 2002. Comparative anatomy of the podocyte: a scanning electron microscopic study. *Microsc Res Tech.* 57:196–202.
- Thisse C, Thisse B. 2008. High-resolution in situ hybridization to whole-mount zebrafish embryos. *Nat Protoc.* 3:59–69.
- Tytler P, Ireland J, Fitches E. 1996. A study of the structure and function of the pronephros in the larvae of the turbot (*Scophthalmus maximus*) and the herring (*Clupea harengus*). *Mar Fresh Behav Physiol.* 28:3–18.
- Wei X, Malicki J. 2002. *nagie oko*, encoding a MAGUK-family protein, is essential for cellular patterning of the retina. *Nat Genet.* 31:150–157.
- Wessely O, Obara T. 2008. Fish and frogs: models for vertebrate cilia signaling. *Front Biosci.* 13:1866–1880.
- Wu J, Janknecht R. 2002. Regulation of the ETS transcription factor ER81 by the 90-kDa ribosomal S6 kinase 1 and protein kinase A. *J Biol Chem.* 277:42669–42679.
- Zhao C, Malicki J. 2007. Genetic defects of pronephric cilia in zebrafish. *Mech Dev.* 124:605–616.
- Zhou W, Boucher RC, Bollig F, Englert C, Hildebrandt F. 2010. Characterization of mesonephric development and regeneration using transgenic zebrafish. *Am J Physiol Renal Physiol.* 299:F1040–F1047.